

## **Electron beam sterilization of poly (methyl methacrylate) - physicochemical and biological aspects**

*Sina Sharifi, Mohammad Mirazul Islam, Hannah Sharifi, Rakibul Islam, Tahmida N. Huq, Per H. Nilsson, Tom Eirik Mollnes, Khoa D. Tran, Corrina Patzer, Claes H. Dohlman, Hiram K. Patra, Eleftherios I. Paschalis, Miguel Gonzalez-Andrades\*, and James Chodosh\**

Dr. S. Sharifi, Dr. M. M. Islam, H. Sharifi, Prof. C. H. Dohlman, Dr. E. Paschalis, Prof. J. Chodosh  
Disruptive Technology Laboratory, Massachusetts Eye and Ear and Schepens Eye Research Institute,  
Department of Ophthalmology, Harvard Medical School, Boston, MA, 02114, USA  
Email: James\_Chodosh@meei.harvard.edu

Dr. Rakibul Islam  
Department of Immunology, Oslo University Hospital, Rikshospitalet, University of Oslo, Oslo, 0424  
Norway

T. N. Huq  
Department of Materials Science and Metallurgy, University of Cambridge, Cambridge, CB3 0FS, UK

Prof. P H. Nilsson  
Department of Immunology, Oslo University Hospital, Rikshospitalet, University of Oslo, Oslo, 0424  
Norway; Linnaeus Center for Biomaterials Chemistry, Linnaeus University, Kalmar, 45027, Sweden

Prof. T. E. Mollnes  
Department of Immunology, Oslo University Hospital, Rikshospitalet, University of Oslo, Oslo, 0424  
Norway; Research Laboratory, Nordland Hospital, Bodø, and Faculty of Health Sciences, K.G. Jebsen  
TREC, University of Tromsø, Tromsø, 9019, Norway; Centre of Molecular Inflammation Research,  
Norwegian University of Science and Technology, Trondheim, 7491, Norway.

Dr. K. D. Tran, C. Patzer  
Vision Research Laboratory, Lions VisionGift, Portland, OR, 97214, USA

Dr. H. K. Patra  
Department of Chemical Engineering and Biotechnology, Cambridge University, Cambridge, CB3  
0AS, UK

Dr. M. Gonzalez-Andrades  
Disruptive Technology Laboratory, Massachusetts Eye and Ear and Schepens Eye Research Institute,  
Department of Ophthalmology, Harvard Medical School, Boston, MA, 02114, USA; Maimonides  
Biomedical Research Institute of Cordoba (IMIBIC), Department of Ophthalmology, Reina Sofia  
University Hospital and University of Cordoba, Cordoba, 14004, Spain  
Email: Miguel.Gonzalez@imibic.org

**Keywords:** poly (methyl methacrylate), electron beam irradiation, sterilization, biocompatibility

Electron beam (E-beam) irradiation is an attractive and efficient method for sterilizing clinically implantable medical devices made of natural and/or synthetic materials such as poly (methyl methacrylate) (PMMA). As ionizing irradiation can affect the physicochemical properties of PMMA, understanding the consequences of E-beam sterilization on the intrinsic properties of PMMA is vital for clinical implementation. We report a detailed assessment of the chemical, optical, mechanical, morphological, and biological properties of medical-grade PMMA after E-beam sterilization at 25 and 50 kiloGray (kGy). Fourier transform infrared spectroscopy, thermogravimetric analysis, and differential scanning calorimetry studies indicate that E-beam irradiation has minimal effect on the chemical properties of the PMMA at these doses. While 25 kGy irradiation does not alter the mechanical and optical properties of the PMMA, 50 kGy reduced the flexural strength and transparency by 10 and 2%, respectively. Atomic force microscopy demonstrates that E-beam irradiation reduces the surface roughness of PMMA in a dose dependent manner. Live-Dead, AlamarBlue, immunocytochemistry, and complement activation studies show that E-beam irradiation up to 50 kGy has no adverse effect on the biocompatibility of the PMMA. These findings suggest that E-beam irradiation at 25 kGy may be a safe and efficient alternative for PMMA sterilization.

## **1. Introduction**

The irradiation of organic polymers intended for medical use with ionizing irradiation such as E-beam often cause the formation of reactive intermediates such as free radicals, ions, and atoms in their excited states.<sup>[1]</sup> These intermediates can undergo various chemical reactions including but not limited to disproportionation, hydrogen abstraction, rearrangements, and breaking and/or formation of new chemical bonds. This is beneficial when it alters the macromolecular structures present in contaminating pathogens, as it eradicates any bio-burden, and sterilizes medical packaging.<sup>[2]</sup> However, such chemical reactions can also modify polymer structures and their properties, depending on the structure of the polymer, exposure dose, duration time, and the irradiation conditions.<sup>[1, 3]</sup> One of the most widely used

polymers in medical technologies and implants is poly (methyl methacrylate) (PMMA). This is due to its excellent biocompatibility, reliability, relative ease of manipulation, and low toxicity.<sup>[4]</sup> Some of the most common application of PMMA in medical technologies are (i) keratoprosthesis,<sup>[5]</sup> (ii) contact and intraocular lens,<sup>[6]</sup> (iii) orthopedic,<sup>[7]</sup> (iv) dental, <sup>[4]</sup> and (v) plastic surgery.<sup>[8]</sup> PMMA-based implants typically come into direct contact with the blood stream or are contained in avascular body compartments and must be sterilized prior to their clinical application.

There are numerous sterilization methods in use including treatment with steam, dry heat, pressured vapor, ethylene oxide (EtO), H<sub>2</sub>O<sub>2</sub> gas plasma, exposing peracetic acid, as well as irradiation— either gamma or E-beam. Effective sterilization must eliminate all infectious agents, including bacteria, viruses, fungi, and parasites, without damaging the intrinsic properties of the material.<sup>[9]</sup> EtO is preferred for sensitive materials that cannot tolerate heat, and thus it is a commonly applied method for sterilization of PMMA-made medical devices,<sup>[10]</sup> for example the Boston keratoprosthesis, a device used to replace a diseased cornea when corneal allograft surgery fails.<sup>[11]</sup> However, EtO sterilization is a slow and expensive process and requires careful handling of EtO due to its toxicity and flammability. Thus, ventilation and aeration are necessary to purge the gas which adds to the cost.<sup>[9]</sup> In contrast, gamma irradiation has been shown to be a feasible and tractable method to sterilize PMMA devices.<sup>[10b, 12]</sup> However, concerns remain around PMMA yellowing when the device is for optical purposes.

E-beam irradiation is an attractive, emission free, and faster sterilization alternative for medical devices, compatible with low temperature requirements for plastics.<sup>[13]</sup> E-beam irradiation allows full control of the dose and temperature during sterilization.<sup>[9]</sup> It has been shown that PMMA can reasonably tolerate a single irradiation sterilization dose, although not repeated sterilizations.<sup>[14]</sup> It was also shown that the E-beam irradiation can affect mechanical and optical properties of industrial PMMA.<sup>[15]</sup> However, whether the level of E-beam irradiation sufficient to achieve sterilization to regulatory standards, induces any clinically relevant effects on the properties of medical-grade PMMA has not been fully studied. The recommended dose for terminal sterilization of medical products is 25 kGy, and

guarantees a Sterility Assurance Level (SAL) of  $10^{-6}$ ,<sup>[9]</sup> herein, we irradiated medical grade PMMA at 25 and 50 kGy and assessed for alteration in chemical, mechanical, morphological, optical, and biological properties of the PMMA to determine the feasibility of using E-beam irradiation for sterilization.

## 2. Results and Discussion

### 2.1. Chemical Characterization

The FT-IR spectra of the PMMA specimens are shown in **Figure 1a**. The FT-IR absorbance spectra of non-irradiated and 25 kGy irradiated PMMA samples are almost superimposable. Yet, upon a closer inspection, it is apparent that the C=C stretching vibration at around  $1637\text{ cm}^{-1}$  grows after irradiation. This coincides with reduction in the intensity of C–O, C=O bonds groups at  $1149$  and  $1731\text{ cm}^{-1}$ , respectively. Such changes in intensities are more predominant with 50 kGy and suggest that as the E-beam dose increases, the rate of chain scission increases to generate free radicals that recombine to form C=C bonds.<sup>[16]</sup> Such reactions deplete the hydrogen from PMMA and transforms the polymer into a hydrogen depleted network as previously suggested.<sup>[17]</sup> Moreover, FT-IR shows a broad low-intensity peak in the higher energy side of the spectra ( $3000\text{--}4000\text{ cm}^{-1}$ ) for PMMA samples after 50 kGy irradiation, suggesting the presence of an OH stretching bond. This may have originated from the oxidative degradation of PMMA during high energy electron bombardment. It was previously shown that electron bombardment generates carbon-centered radicals that can either react with each other to form a crosslinked network or react with atmospheric oxygen to produce peroxy radicals, which can act as initiator to induce various reactions or can form stable products including hydroxyl bearing functional groups.<sup>[16, 18]</sup>

To confirm surface oxidation, we also performed X-ray photoelectron spectroscopy (XPS). Our data shows that E-beam irradiation decreases C/O atomic ratio from 2.62 (PMMA) to 2.49 (25 kGy) and 2.33 (50 kGy) as tabulated in **Table S1**. While 25 kGy irradiation decreases the C–O–C atomic ratio and

maintains the  $\text{C}=\text{O}$  atomic ratio, 50 kGy decreases both  $\text{C}-\text{O}-\text{C}$  and  $\text{C}=\text{O}$  atomic ratios. The former suggests transformation of ester functionality to carboxylic acid, and the later suggests the loss of small gaseous molecules, such as CO and CO<sub>2</sub>, as also proposed by others after irradiation PMMA film with low energy electrons.<sup>[19]</sup> However, 50 kGy irradiation also increases the  $\text{C}-\text{OH}$  atomic ratio, indicating the addition of hydroxyl groups onto the surface of the PMMA (**Figure S2-S3**). These data suggest that the higher doses of irradiation have a more pronounced effect on the chemical structure of PMMA.

The TGA and TGA-derivative plots of non-irradiated and irradiated (25 and 50 kGy) PMMA are co-plotted in **Figure 1b**. As shown in **Figure 1** and **Table 1**, the irradiation of PMMA with 25 and 50 kGy reduces the onset temperature ( $T_{10}$ : temperature at 10% mass loss) from 273.4 to 236.4 and 238.4 °C, respectively. This coincides with the first decomposition stage of the PMMA as indicated by the appearance of the TGA derivative peak at 228.8 and 224.2 °C. This finding is believed to be originated from the presence of lower molecular weight and unstable fragments in irradiated PMMA that undergo degradation and evaporation at lower temperatures, as compared to non-irradiated PMMA, in which there was no such change.<sup>[20]</sup> Lower doses of irradiation (25 kGy) appeared to decrease the onset temperature more than those of higher doses (50 kGy). On the other hand, the midpoint temperature ( $T_{50}$ : temperature at 50% mass loss) drops for 25 kGy but increases for 50 kGy. This suggests that at a lower dose of irradiation, chain scission dominates the degradation processes, while at a higher dose, crosslinking of the generated reactive species may occur. Such chain scission and crosslinking are also responsible for reducing and increasing  $T_{\text{max}}$  (maximum weight loss temperature) in 25 kGy and 50 kGy irradiated PMMA, respectively. Although the thermal behavior of PMMA after E-beam irradiation with varying doses has not been previously studied, prior studies of gamma irradiated PMMA showed similar behavior.<sup>[21]</sup>

**Table 1:** Data Obtained from TGA and DSC Thermograms

Samples	TGA				DCS
	$T_{10}$ (°C)	$T_{50}$ (°C)	$T_{\text{max}}$ / °C (°C)		$T_g$ (°C)
			Stage 1	Stage 2	

PMMA	273.4	340.0	-	349.1	131.1
25 kGy	236.4	337.8	228.8	347.9	128.2
50 kGy	238.4	342.8	224.2	353.6	128.3

The DSC thermograms of non-irradiated, 25 and 50 kGy irradiated PMMA along with their corresponding glass transition temperature ( $T_g$ ), are shown in **Figure 1c**. E-beam irradiation of PMMA shifted the  $T_g$  from 131.1 °C to 128.2 °C and 128.3 °C for 25 and 50 kGy respectively, and altered the slope of heat flow in the DSC curves. The former suggests increase in the mobility of the polymer chains, and the latter indicates the presence of smaller molecular weight species which then can undergo degradation or evaporation.<sup>[22]</sup> This is in agreement with the TGA studies, validating the dominance of chain scission and crosslinking for 25 and 50 kGy, respectively. Although data suggest that E-beam irradiation affects the thermal properties of the PMMA, this is biologically insignificant, considering that PMMA implants reside at body temperature (37 °C).

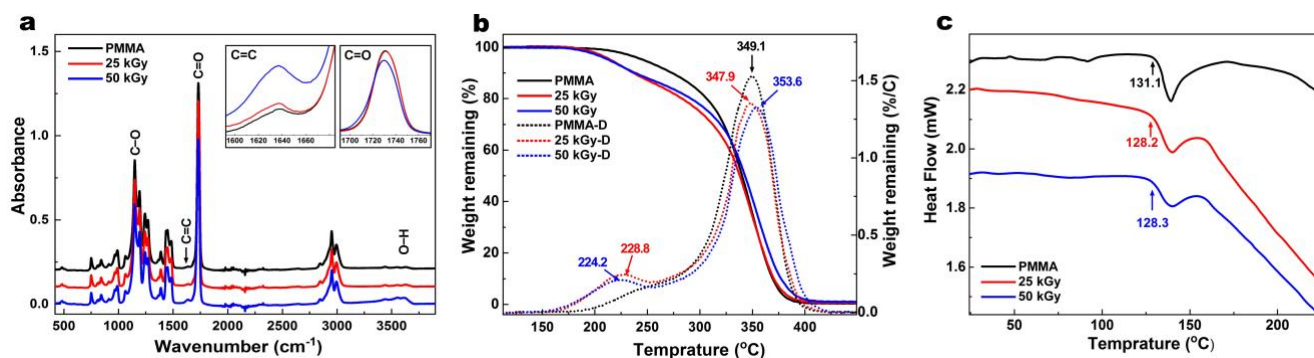


**Figure 1.** Chemical characterization of PMMA after E-beam irradiation. (a) Fourier transform infrared (FT-IR) spectra, (b) Thermal Gravimetric analysis (TGA), and (c) Differential scanning calorimetry (DSC) plots of PMMA before and after 25 or 50 kGy irradiation. Increasing C=C and O-H and reducing C=O and C-O peaks intensities suggest that 50 kGy has a more prominent effect on the chemical structure of the PMMA. Irradiated samples have two decomposition stages compared to one in non-irradiated PMMA, with varying  $T_{10}$ ,  $T_{50}$ ,  $T_{max}$ , (TGA) and  $T_g$  (DSC), suggesting the chain scission and crosslinking in the 25 and 50 kGy, respectively.

## 2.2. Mechanical Characterization

To determine whether the E-beam irradiation impacts the mechanical properties of the PMMA, we performed 3-point bending test (**Figure 2a**) and calculated flexural modulus and strength according to a previously described approach.<sup>[23]</sup> **Figure 1b-d** represents the flexural strains for non-irradiated, 25, and 50 kGy irradiated PMMA discs as function of stress. Our data shows that the flexural modulus of non-irradiated, 25, and 50 kGy irradiated PMMA is  $5.46 \pm 0.48$ ,  $5.22 \pm 0.35$  and  $5.10 \pm 0.37$  GPa, respectively (**Figure 1e**). Although the apparent gradual decrease in the flexural modulus of PMMA is consistent with a prior study,<sup>[15]</sup> statistical analysis showed no significant difference between the irradiated and non-irradiated PMMA ( $p > 0.05$  for both comparisons). Moreover, 25 and 50 kGy irradiated PMMA samples demonstrate a flexural strength of  $0.456 \pm 0.024$  and  $0.427 \pm 0.025$  GPa, respectively, as compared to  $0.470 \pm 0.033$  GPa of non-irradiated PMMA (**Figure 2f**). These data suggest that only the 50 kGy dose was statistically different from non-irradiated PMMA ( $p = 0.012$ ). Thus, irradiation at 25 kGy with E-beam did not significantly change the mechanical properties of PMMA.

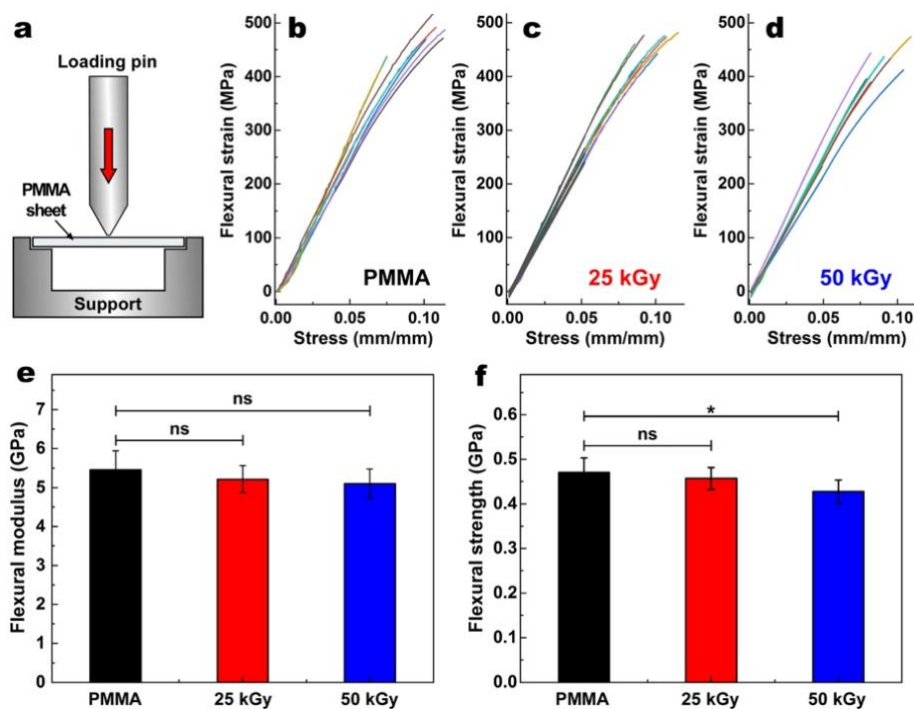


**Figure 2.** Schematic illustration of standard three-point bending flexure test (**a**). Obtained flexural strain as function of stress for non-irradiated (**b**), 25 kGy (**c**) and 50 kGy (**d**) irradiated PMMA and their corresponding flexural moduli (**e**) and flexural strengths (**f**). There was no significant difference in flexural modulus between non-irradiated and 25 and 50 kGy PMMA. ns, and \* represent  $p > 0.05$ ,  $p \leq 0.05$ , respectively. Values are presented as mean  $\pm$  SD; n = 8.

### 2.3. Optical Properties

Optical transmission studies of PMMA discs before and after E-beam irradiation using UV-Vis spectroscopy show that the E-beam irradiation reduces the optical transmission of PMMA in a dose-dependent manner, as illustrated in **Figure 3a-d**. The reduction of transmission in the visible range (390-490 nm) was  $2.7 \pm 0.2 \%$  and  $6.2 \pm 0.3 \%$  for 25 and 50 kGy irradiated PMMA, respectively. However, those reductions were more pronounced  $52.7 \pm 0.8 \%$  and  $67.6 \pm 1.1 \%$  in the ultraviolet (UV) region of spectra (250-350 nm) for 25 and 50 kGy, respectively. The E-beam treatment also results in reduction of light transmission in the visible range (390-490 nm) and consequently yellowing of the PMMA samples. However, the yellowing effect gradually fades away at room temperature within the first 30 days after irradiation (**Figure 3**), and then the color remains stable for both 25 and 50 kGy samples. While light transmission in the visible range recovered fully in the 25 kGy group, in the 50 kGy group it failed to recover (**Figure 3d**). The recovery rate in the UV range was dose-dependent, and neither of the two groups (25 and 50 kGy) achieved full recovery. The reduction in transmission originates from the changes in the chemical structure of the PMMA, as indicated by FT-IR, DSC, and TGA studies. While 25 kGy irradiation does not affect the transmission of visible light, but it stably reduces the transmission of harmful UV light, which could be beneficial for device recipients. This is due to the fact that UV light elicits phototoxicity and was shown to induce reactive oxygen species (ROS) production in the aqueous humor, damage mitochondrial DNA (mtDNA) and nuclear DNA (nDNA) in the endothelial cells, and cause corneal endothelial cell loss, leading to corneal edema.<sup>[24]</sup> Moreover, UV light can cause photochemical damage in retinal cells through (*i*) direct reactions involving proton or



electron transfers and (ii) reactions involving reactive oxygen species mechanisms.<sup>[25]</sup> The 50 kGy irradiation of PMMA, on the other hand, stably reduces the light transmission in the visible and UV range. In comparison, a similar dose of gamma irradiation (25 kGy) shows a significantly greater impact on the optical properties of PMMA, and reduced transmission in the visible range of 350-500 nm by  $15.0 \pm 0.5\%$  with only  $3.0 \pm 0.1\%$  recovery in 90 days.<sup>[10b]</sup>

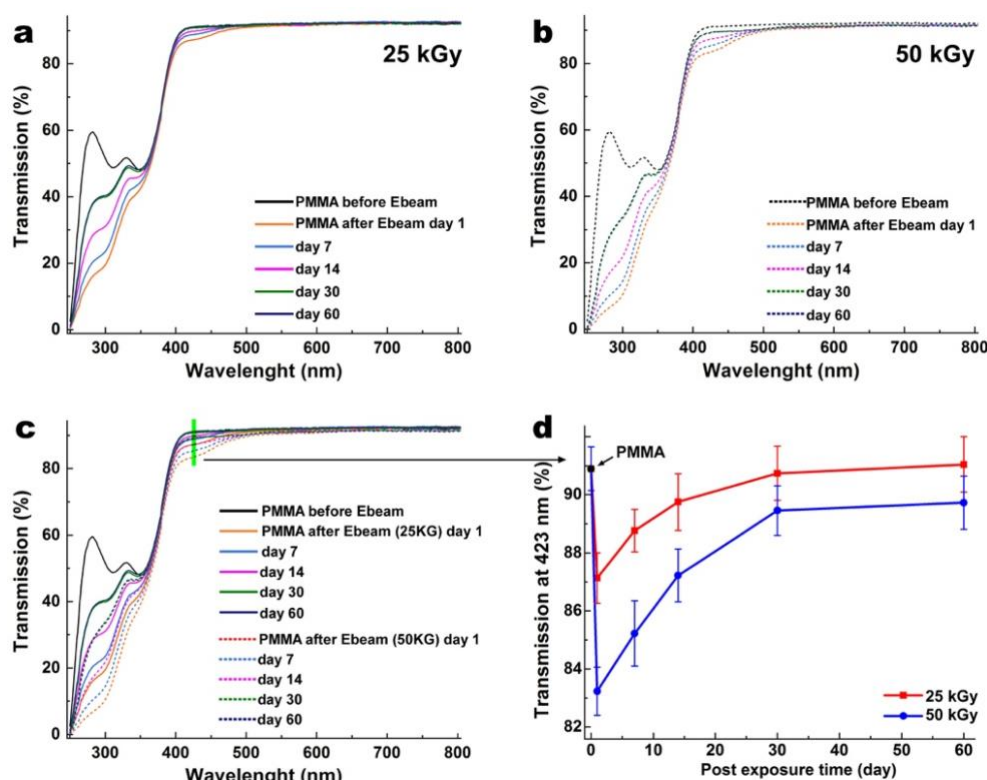


**Figure 3.** Graphs of optical transmission of PMMA before and after irradiation at 25 kGy (a), 50 kGy (b), and with both superimposed (c) as a function of time to 60 days post treatment, in the range on 250-800 nm. d) The recovery of transmission plotted at 423 nm (extracted from (c) plot, as shown by green line) after 25 and 50 kGy irradiation. 25 kGy irradiated PMMA samples reach near full recovery after 1 month. The 50 kGy irradiated PMMA recovered 95% of transmission in the blue light area. Data are presented as mean  $\pm$  SD; n = 4.

## 2.4. Surface Properties

Bombardment of the PMMA surface with high energy E-beam irradiation has shown to alter the crosslinking density and chemical and morphologic characteristics of PMMA films, potentially leading to amorphization.<sup>[17, 26]</sup> To investigate whether E-beam irradiation impacts the morphological properties of medical-grade PMMA, we employed an AFM study. Our data demonstrate a dose dependent smoothing of the surface after irradiation (Figure 4a-c). The surface roughness analysis showed Root Mean Square (RMS) values of  $9.34 \pm 2.39$ ,  $7.15 \pm 1.42$ , and  $5.92 \pm 1.79$  for non-irradiated, 25 kGy, and 50 kGy irradiated PMMA, respectively, demonstrating that irradiation reduced surface roughness (Figure 4d). We performed water contact angle measurements to determine whether E-beam irradiation has affected the wettability of the PMMA surface. This analysis showed reductions in the water contact angle from  $74.5 \pm 3.2^\circ$  for non-irradiated PMMA to  $66.7 \pm 2.5^\circ$ , and  $62.6 \pm 3.1^\circ$  for 25 and 50 kGy irradiated samples, respectively (Figure 4e). These changes could originate from oxidation of the PMMA surface and formation of hydroxyl group, as shown by XPS, along with the changes in the morphological properties due to electron bombardment.<sup>[27]</sup>

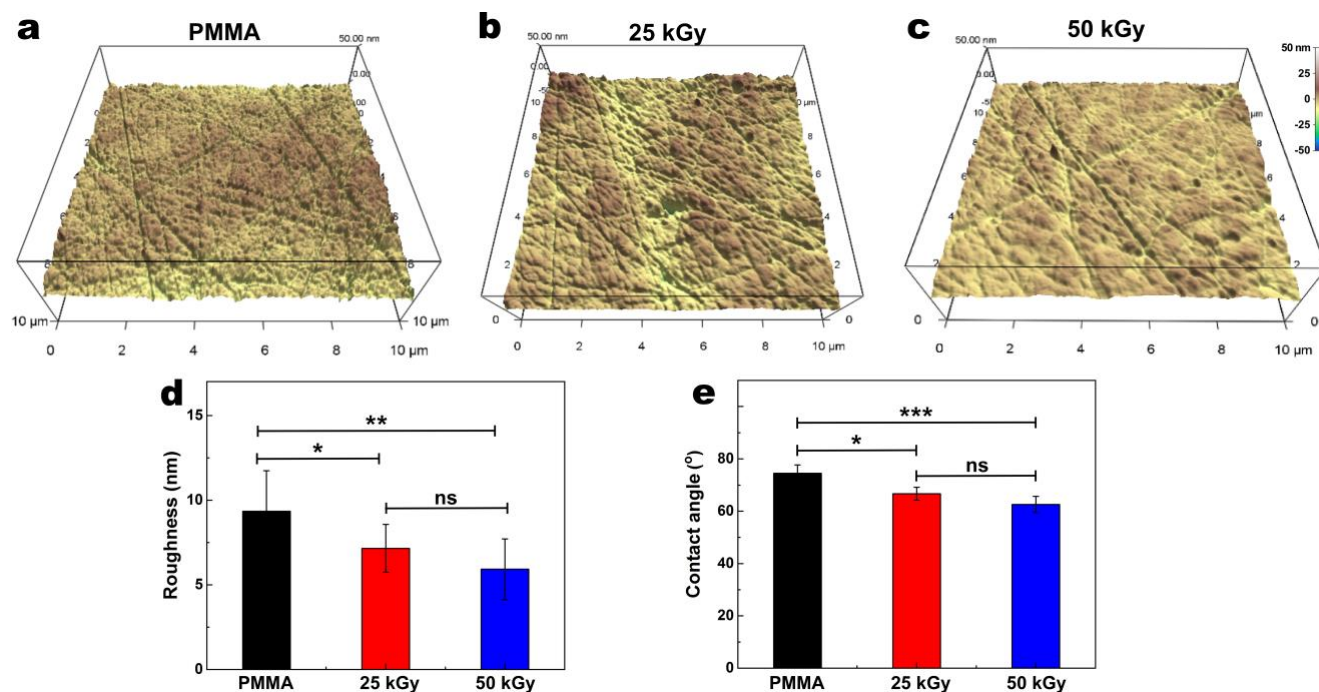


**Figure 4.** Morphological characterization of PMMA surface before (a), after 25 kGy (b), and 50 kGy (c) irradiation with a scan size of  $10 \times 10 \mu\text{m}^2$  and their analyzed surface roughness (d), using Atomic Force Microscopy (AFM). (e) contact angle values of PMMA surfaces before, and after 25 kGy and 50 kGy irradiation. AFM and contact angle studies suggested that irradiation decreases the roughness and contact angle in a dose dependent manner. ns, \*, and \*\* represent  $p > 0.05$ ,  $p \leq 0.05$ , and  $p \leq 0.01$ , respectively. Data are presented as mean  $\pm$  SD; n = 5.

## 2.5. Biocompatibility

Since E-beam irradiation alters the structure and surface properties of PMMA, we assessed the effect of these changes on cytotoxicity and biocompatibility of the PMMA. After culturing human corneal fibroblasts (HCF) on non-irradiated or irradiated PMMA discs (25, and 50 kGy), we performed a Live-Dead assay and studied the cell viability (**Figure 5a-b**). In the Live-Dead assay live cells stain with green-fluorescent calcein-AM on the basis of ongoing intracellular esterase activity, while dead cells with red-fluorescent ethidium homodimer-1 because of loss of plasma membrane integrity. Therefore, this assay enables estimation of cell viability within a cell population.<sup>[28]</sup> Live-Dead analysis (**Figure 5b**) showed no significant differences between cell viability of non-irradiated, 25, and 50 kGy PMMA discs during 7 days of cell culture ( $> 90\%$ ), suggesting that irradiation did not produce cytotoxic products, which otherwise would affect the cells viabilities. Moreover, cells cultured on all three groups had similar cell morphologies and spreading patterns indicating similar biocompatibility.<sup>[29]</sup> We also studied the interaction of human corneal epithelial cells (HCEp) with PMMA with and without E-beam irradiation (**Figure 5c-d**). HCEp seeded on non-irradiated, 25, and 50 kGy irradiated PMMA samples demonstrated similar morphology and viability ( $> 85\%$ ) over 7 days of culture (**Figure 5d**). These data suggest that E-beam irradiation of PMMA does not induce cytotoxicity or reduce its biocompatibility.

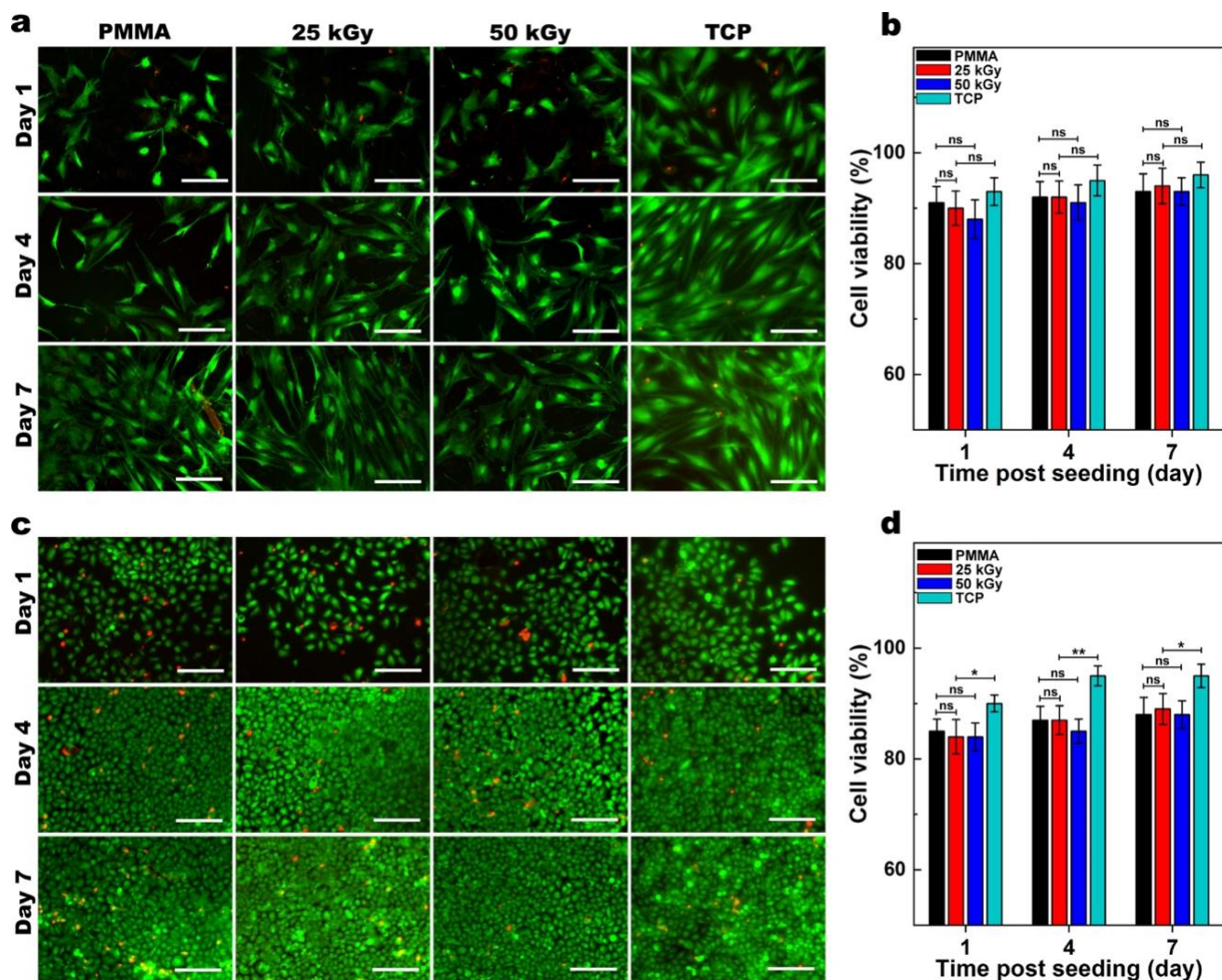


**Figure 5.** Biocompatibility of PMMA with and without E-beam irradiation. Representative Live/Dead images of human corneal fibroblasts (HCF) (a) and human corneal epithelial (HCEp) cells (c) cultured on PMMA, with and without 25 or 50 kGy irradiation compared to those cultured on tissue culture plates (TCP), and their corresponding cell viability (b and d) after 1, 4, and 7 days of cell culture (scale bar: 200  $\mu$ m). Cells viability was quantified from Live/Dead images using ImageJ (Green [calcein AM]: lived cells; Red [ethidium homodimer-1]: dead cells). Values are presented as mean  $\pm$  SD; n = 4. ns, \*, \*\*, \*\*\*, and \*\*\*\* represent  $p > 0.05$ ,  $p \leq 0.05$ ,  $p \leq 0.01$ ,  $p \leq 0.001$  and  $p \leq 0.0001$ .

We further studied the metabolic activity of HCF and HCEp seeded on PMMA with or without irradiation using the AlamarBlue assay. A steady increase in the relative metabolic activity as function of incubation time suggests cellular growth and proliferation over time on all samples. At days 1, 3, and 7, of cell culture, HCF and HCEp grown on 25 and 50 kGy PMMA discs had similar activity to those on

non-irradiated PMMA (**Figure 6**). These results are consistent with the Live-Dead assays and indicate that 25 and 50 kGy E-beam irradiation do not adversely affect PMMA biocompatibility.

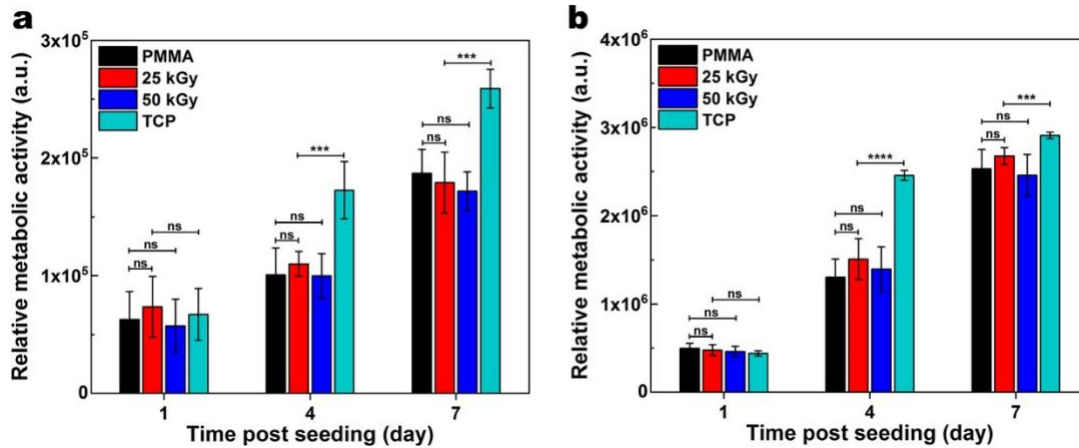


**Figure 6.** Quantification of the metabolic activity of HCF (a), and HCEp (b) cultured on PMMA, with or without 25 and 50 kGy irradiation compared to those cultured on tissue culture plate (TCP), using AlamarBlue assay performed at 1, 4, and 7 days of cell culture. The cells seeded on all three surfaces demonstrated similar metabolic activity, suggesting that the irradiation did not diminish biocompatibility of the PMMA. Data are presented as mean  $\pm$  SD; n = 12. ns, \*, \*\*, \*\*\*, and \*\*\*\* represent  $p > 0.05$ ,  $p \leq 0.05$ ,  $p \leq 0.01$ ,  $p \leq 0.001$  and  $p \leq 0.0001$ .

## 2.6. Immunocytochemistry (ICC)

To assess the interaction of HCF with E-beam irradiated PMMA, we also studied the expression of specific cellular markers, including those indicative of adhesion, proliferation, and inflammation (**Figure 7**) using ICC. ALDH3A1 (keratocyte specific marker) expression was limited on both non-irradiated and irradiated (25 and 50 kGy) PMMA as previously shown<sup>[30]</sup>. Moreover, the expression of focal adhesion kinase (FAK), which is associated with cellular adhesion and spreading was similar for cells grown on non-irradiated and irradiated PMMA. The expression of integrin  $\beta$ 1, which is associated with the cellular adhesion and interaction with the surrounding extra cellular matrix is also similar between groups. Thus, these expression patterns indicate that E-beam irradiation does not adversely impact cellular adhesion, or proliferation and spreading of HCF on PMMA. In addition, most HCF cultured on both non-irradiated and irradiated (25 and 50 kGy) PMMA expressed  $\alpha$ -SMA, indicating a myofibroblast phenotype, which can be associated with fibrotic responses.<sup>[31]</sup>

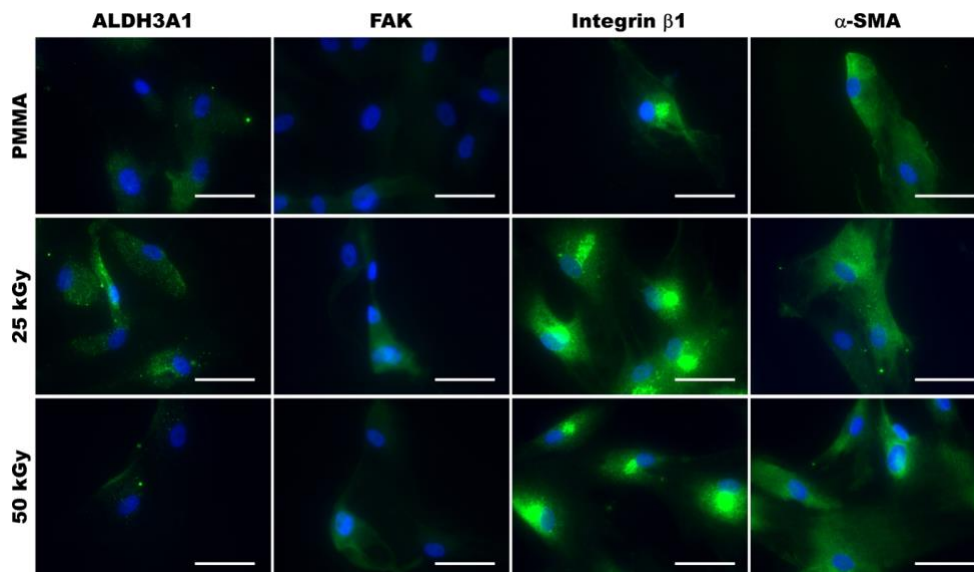


**Figure 7.** Representative immunofluorescence images of HCF cultured on non-irradiated or E-beam irradiated (25 and 50 kGy) PMMA for 7 days, and immunostained for ALDH3A1, focal adhesion kinase (FAK), integrin  $\beta$ 1, and smooth muscle actin ( $\alpha$ -SMA). Minimal variations were observed between cells grown on non-irradiated and irradiated PMMA. All cell nuclei were counterstained using DAPI (blue). Scale bar is 50  $\mu$ m.

## 2.7. Complement Activation

Implanted materials were exposed to recognition molecules of the innate immune system in plasma cascades, of which the complement system is a central component, playing a key role in homeostasis, regeneration, and inflammation.<sup>[32]</sup> To assess complement activation, two activation fragments of the complement system were studied, C3bc and TCC (**Figure 8**). C3bc levels were similar between non-irradiated, and irradiated (25 and 50 kGy) PMMA, and to the background activation after 30 min incubation without PMMA (T30), but higher in comparison to the plasma levels immediately after blood draw (T0) ( $p \leq 0.05$ ), as illustrated in **Figure 8a**. Soluble TCC levels were also similar between non-irradiated, irradiated (25 and 50 kGy) PMMA, and T30, and higher than at T0 ( $p \leq 0.0001$ ) (**Figure 8b**). These data suggest that although PMMA induces a low-grade complement activation, the E-beam irradiation has no impact on its complement activating properties.

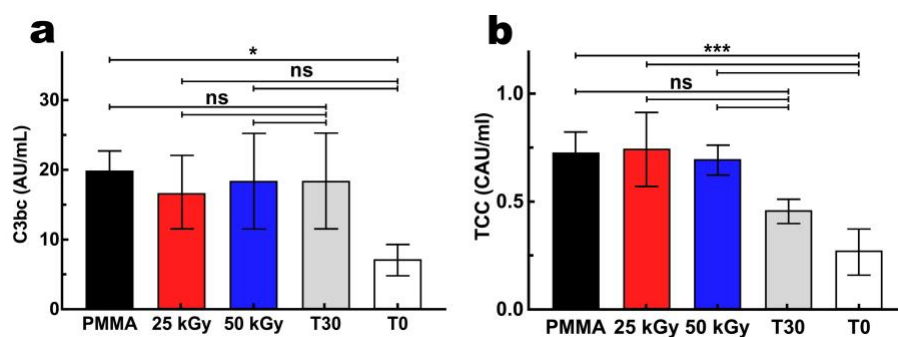


**Figure 8.** Complement activation of C3bc (a) and soluble terminal complement complex (TCC) (b) with or without E-beam irradiation compared to the background activation without PMMA after 30 minutes (T30), and the level at the start of incubation (T0). The level of C3bc was statistically different only for T0; the latter represents the status of complement activation immediately after drawing blood from the donor. Values are presented as mean  $\pm$  SD; n = 4. ns ( $p > 0.05$ ), \* $p \leq 0.05$ , \*\* $p \leq 0.01$ , \*\*\* $p \leq 0.001$ , and \*\*\*\* $p \leq 0.0001$ .

### 3. Conclusion

In summary, we have shown that 25 kGy E-beam irradiation has a minimal impact on the chemical, mechanical, and optical properties of PMMA and has no apparent adverse effect on its biocompatibility with human corneal cells. These findings suggest that 25 kGy E-beam irradiation may be a feasible sterilization alternative for PMMA used in medical implants. Future studies are required to determine the effect of E-beam sterilization *in vivo*.

### 4. Experimental Section

**E-beam Irradiation:** Medical grade PMMA (Rod number 2, PolyOne; Littleton, MA) discs with 0.5 mm thickness and 40.0 mm diameter were acquired from JG Machine Company (Wilmington, MA). The PMMA discs were placed and sealed in Medical Pouches (Steriking SS-T 4A; Helsinki, Finland), placed on an aluminum carrier tray, and irradiated using a Van de Graaff (Model K) electron accelerator (Electron Technology Company; South Windsor, CT) at 2.6 Mev with the dose rate of 5 kGy per pass (5, and 10 passes to reach 25 and 50 kGy irradiation, respectively).

*Fourier Transform Infrared Spectroscopy (FT-IR):* FT-IR spectra of the PMMA discs (non-irradiated, 25 and 50 KGy irradiated) were collected in the range from 500 to 4000  $\text{cm}^{-1}$  using a Nicolet iS50 FT-IR Spectrometer (Thermo Scientific; Waltham, MA) equipped with all-reflective diamond Attenuated Total Reflectance (ATR). Spectra were acquired and analyzed *via* OMNIC software (Thermo Scientific) with 64 scans and 0.5  $\text{cm}^{-1}$  resolution after spectral correction with ambient atmosphere.

*X-ray Photoelectron Spectroscopy (XPS):* XPS spectra of the PMMA discs (non-irradiated, 25 and 50 KGy irradiated) were obtained in the range of 0 to 1300 eV with an energy step size of 1 eV using a Thermo Scientific K-Alpha (Thermo Scientific, Waltham, MA). The spectra were acquired and analyzed *via* Avantage software (Thermo Scientific) in both survey and high-resolution modes. The high-resolution XPS spectra of C and O were deconvoluted using Avantage software with Simplex fitting algorithm and Gaussian–Lorentzian product function.

*Water Contact Angle Measurement:* The contact angle measurements were carried out by a Contact Angle and Surface Tension Measurement System (FTA100, First Ten Angstroms, Portsmouth, VA) using a static sessile drop technique. At room temperature, 5  $\mu\text{L}$  size drop of distilled water was placed by a syringe, located above the sample surface, and then a high-resolution camera used to capture an image from the side. The contact angle was analyzed and recorded using FTA 2.1 software and averaged for each group [n = 4].

*Optical Transmission:* The light transmission of the PMMA discs (0, 25 and 50 KGy irradiated) was assessed by a UV-Vis spectrometer (Molecular Devices SpectraMax 384 Plus Microplate Reader; Molecular Devices, San Jose, CA). Briefly, PMMA discs were cut to 6.0 mm diameter by a laser cutter (Helix 75W Laser Cutter; Epilog, Golden, CO), and placed in a 96-well quartz microplate to record their optical transmittance from 250-850 nm in a quartz microplate at 1-nm wavelength increments at varying time points (1-60 days) after irradiation. The transmittance of the samples [n = 4] was corrected with blank media (air) and the mean transmittance (%) for each group was calculated and plotted as a function of wavelength.



*Atomic Force Microscopy (AFM):* The morphology of the PMMA discs (0, 25 and 50 KGy irradiated) was scanned by an AFM instrument (Asylum Research Cypher - Oxford Instruments, High Wycombe, UK) in the AC mode. The data was acquired in phase and height profiles with scan size of  $10 \times 10 \mu\text{m}^2$  and rate of 2.0 Hz.

*Thermal Gravimetric Analysis (TGA):* TGA was performed using a TA Instruments TGA Q50 (New Castle, DE). Samples weighing between 2.3-3.5 mg, were initially heated in a platinum pan at a rate of  $10 \text{ }^\circ\text{C}/\text{min}$  to reach  $100 \text{ }^\circ\text{C}$ , and kept isothermal for 15 mins in argon with a flow rate of  $80 \text{ mL}/\text{min}$ . The temperature was then increased to  $600 \text{ }^\circ\text{C}$  at a rate of  $20 \text{ }^\circ\text{C}/\text{min}$  under argon.

*Differential Scanning Calorimetry (DSC):* DSC measurements were performed using a TA Instruments DSC Q20 thermal analyser (New Castle, DE). The PMMA samples were cut into 4.0 mm diameter discs, weighed using a Sartorius balance (Göttingen, Germany), and encapsulated in crimped aluminium pans. An empty pan was used as a reference. The temperature system was allowed to equilibrate at  $0^\circ \text{C}$  and remained isothermal for 10 mins before being ramped to  $250^\circ \text{C}$  at  $10 \text{ }^\circ\text{C}/\text{min}$  under an argon flow of  $80 \text{ ml}/\text{min}$ .

*Mechanical Properties:* The mechanical properties of PMMA before and after varying E-beam irradiation were assessed using standard three-point bending flexure test.<sup>[23]</sup> Briefly, PMMA discs (0, 25 and 50 KGy irradiated) were cut to rectangular shapes ( $15 \times 4 \text{ mm}$ ) with the thickness of 0.5 mm using a Helix 75W laser cutter, then placed on the two-point holder and fixed on the stationary stage of a mechanical tester (Mark-10 ESM 303; Copiague, NY). A longitudinal downward force was applied using the flathead loading pin from the mobile stage with crosshead speed of  $2 \text{ mm}/\text{min}$ . The applied force as a function of displacement was recorded and used to calculate the flexural modulus and strength of the specimens [ $n = 8$ ].

*Live-Dead Assay:* To assess the biocompatibility of the PMMA before and after E-beam irradiation with respect to human corneal fibroblasts (HCF) and human corneal epithelial cells (HCEp), we performed a

standard Live-Dead assay. After E-beam irradiation of 8.0 mm PMMA discs, they were placed in a 48-well cell culture plates and washed with sterile phosphate buffered saline (PBS). Next, HCF (10,000) or HCEp (5000) were seeded on each disc suspended in 20  $\mu$ L of respective media (*i.e.* HCF: low glucose DMEM media (Gibco; Gaithersburg, MD) supplemented 1mM of L-ascorbic acid 2-phosphate (Sigma-Aldrich, St. Louis, MO), 1x Insulin-Transferrin-Selenium Supplement (ITS; Sigma-Aldrich), 1% Glutamax (Gibco), 1x penicillin/streptomycin (Gibco), 1g/L of D-glucose (Sigma-Aldrich), and 2.5 g/L of D-mannitol (Sigma-Aldrich); and HCEp: serum-free medium (KSFM) supplemented with 50  $\mu$ g/ml bovine pituitary extract and 5 ng/ml epidermal growth factor (Gibco)) and allowed to adhere for 30 min prior to addition of 500  $\mu$ L of extra media,<sup>[10b, 33]</sup> followed by incubation at 37 °C and 5% CO<sub>2</sub> for up to 7 days. The respective culture media was changed every other day. Following 1, 4, and 7 days of cell culture, Live-Dead staining was performed according to the manufacturer's instructions (Life Technologies Carlsbad, CA) and imaged using an inverted fluorescent microscope (Zeiss Axio Observer Z1; Thornwood, NY). Four samples per group (25 and 50 kGy) were examined and compared to those of tissue culture well plate (TCP) and non-irradiated PMMA discs as controls. Cellular viability was analyzed using ImageJ software (NIH, Bethesda, Maryland) from images obtained from each sample (n = 4), as described previously.<sup>[30, 34]</sup>

*AlamarBlue Assay:* Standard AlamarBlue assay was performed to evaluate the metabolic activity of the HCF and HCEp seeded on the PMMA discs (0, 25 and 50 kGy irradiated). After culturing the cells on the discs, as explained above, the AlamarBlue study was carried out at days 1, 4, and 7 post-seeding. At each time point, the discs were transfer to a new well and 300 $\mu$ L cell culture media containing 0.0004% resazurin sodium salt (Sigma-Aldrich) was added and incubated for 4 h at 37 °C. Next, 300  $\mu$ L of the same media was transferred to a new 96 well plate (100  $\mu$ L in each well) and read on a BioTek plate reader (Synergy 2, BioTek Instruments) at 530/25 nm for excitation and 600/25 nm for emission, and corrected for the fluorescence of discs incubated without cells. Twelve samples per group (25 and 50

kGy) were tested and compared to those of TCP and non-irradiated PMMA discs as controls. Discs were discarded after each time point.

*Immunocytochemistry (ICC):* Specific markers (ALDH3A1, integrin  $\beta$ 1, FAK and  $\alpha$ -SMA) expressed by HCF seeded on PMMA substrates (non-irradiated, 25 and 50 KGy) were assessed by fluorescence ICC. After culturing cells on the PMMA discs for 6 days as above, the discs were removed from the media, gently washed with PBS, and fixed with 4% paraformaldehyde. Fixed cells were permeabilized with 0.25% Triton X-100 and treated with 5% Fetal bovine serum in PBS with 0.05% Tween-20 (PBST), followed by incubation with primary antibodies overnight at 4 °C in humidifying conditions. The specific antibodies included: (i) mouse monoclonal antibody against ALDH3A1 (clone 1B6; GTX84889, dilution 1:100, GenTex); (ii) rabbit polyclonal antibody against Integrin  $\beta$ 1 (GTX112971, dilution 1:250, GenTex); (iii) rabbit monoclonal antibody against FAK (clone EP695Y; ab40794, dilution 1:250, Abcam); and (iv) mouse monoclonal antibody against  $\alpha$ -SMA (clone 1A4; ab7817, dilution 1:200, Abcam). Subsequently, the specimens were incubated with FITC-conjugated anti-mouse antibody (ab6785, dilution 1:1000, Abcam), or FITC-conjugated anti-rabbit antibody (ab6717, dilution 1:1000, Abcam) for 1h at room temperature, mounted in VectaShield mounting media containing DAPI (Vector Laboratories) and imaged by an inverted fluorescent microscope (Zeiss Axio Observer Z1).

*Ex-Vivo Complement Activation:* Activation of complement by PMMA before and after irradiation was assessed as previously described, using blood from human donors.<sup>[35]</sup> The ethical committee at Oslo University Hospital approved the study (REK SØR S-04114), and the research conformed to the Declaration of Helsinki. Informed written consent was obtained from each donor. Human blood was drawn from healthy volunteers into Vacutainer™ tubes (Becton, Dickinson and Co., Plymouth, UK) containing a specific thrombin inhibitor, lepirudin (Refludan®, Celgene, Uxbridge, UK) at a final concentration of 50  $\mu$ g/mL. For each set of experiments, 300  $\mu$ L of the blood was aliquoted into five cryogenic vials (Thermofisher, MA). In one vial, EDTA was added immediately at 10 mM final

concentration to measure the complement activation status at time zero (T0). The other four vials containing whole blood were incubated at 37 °C as follows: non-irradiated, 25, and 50 kGy irradiated PMMA discs were each placed in a vial. The fourth vial was left with only whole blood. After incubation, EDTA was added to stop further complement activation, and plasma was separated for preservation. The incubated whole blood without an immersed specimen served as a negative control for complement activation. A total of five independent experiments were performed at 30 minutes incubation. Collected plasma was preserved at -70 °C. Complement activation was assessed by measuring soluble C3bc fragments, and the soluble terminal complement complex sC5b-9 (TCC), both using ELISA as described previously.<sup>[36]</sup> The C3bc content was determined using monoclonal antibody bH6 for capture and polyclonal rabbit anti-C3c (Behringwerke AG, Marburg, Germany) and peroxidase-labeled anti-rabbit immunoglobulin (GE Healthcare, Chicago, IL) for detection. Levels of sC5b-9 were determined with anti-neo C9 monoclonal antibody aE11 for capture,<sup>[37]</sup> and biotinylated monoclonal anti-C6 (clone 9C4) as previously described.<sup>[36-37]</sup> Streptavidin-HRP conjugate (GE Healthcare, Chicago, IL) was added for detection.

*Statistical Analysis:* One-way ANOVA with Tukey comparison test was used to compare flexural strain and modulus surface roughness, contact angle, viability, metabolic activity, and TCC between groups. A value of  $p \leq 0.05$  was considered statistically significant. n.s., \*, \*\*, \*\*\*, and \*\*\*\* represent  $p > 0.05$ ,  $p \leq 0.05$ ,  $p \leq 0.01$ ,  $p \leq 0.001$  and  $p \leq 0.0001$ , respectively. GraphPad Prism Software (GraphPad Software version 8.3.0, CA, USA) was used to analyze the data.

### **Supporting Information**

Supporting Information is available from the Wiley Online Library or from the author.

### **Acknowledgements**

This work was supported by a Barbara L. Crow Investigator-Concept Grant from Lions VisionGift, Portland, Oregon, and Boston Keratoprosthesis. R.S. was supported in part by EBAA/ Richard Lindstrom Research Grant (530720), and by a grant from NIH, K99 EY030553. T.N.H. acknowledges

funding from the EPSRC Centre for Doctoral Training in Graphene Technology (No. EP/L016087/1) and the Aziz Foundation. This work was performed in part at the Center for Nanoscale Systems (CNS), Harvard University, a member of the National Nanotechnology Coordinated Infrastructure Network (NNCI), which is supported by the National Science Foundation under NSF award no. 1541959.

Received:

Revised:

Published online:

## References

- [1] M. Haji-Saeid, M. H. O. Sampa, A. G. Chmielewski, *Radiat. Phys. Chem.* **2007**, 76, 1535.
- [2] L. Woo, C. L. Sandford, *Radiat. Phys. Chem.* **2002**, 63, 845.
- [3] a) J. G. Drobny, in *Ionizing Radiation and Polymers*, DOI: <https://doi.org/10.1016/B978-1-4557-7881-2.00002-X> (Ed: J. G. Drobny), William Andrew Publishing **2013**, p. 11; b) A. Chapiro, *Nuclear Instruments and Methods in Physics Research Section B: Beam Interactions with Materials and Atoms* **1988**, 32, 111.
- [4] R. G. Hill, in *Biomaterials, artificial organs and tissue engineering* (Eds: L. L. Hench, J. R. Jones), Woodhead Publishing, England **2005**, Ch. 10, p. 97.
- [5] a) B. F. Khan, M. Harissi-Dagher, D. M. Khan, C. H. Dohlman, *Int Ophthalmol Clin* **2007**, 47, 61; b) S. Pujari, S. S. Siddique, C. H. Dohlman, J. Chodosh, *Cornea* **2011**, 30, 1298.
- [6] D. A. Atchison, *J Cataract Refract Surg* **1990**, 16, 178.
- [7] a) G. Lewis, *Journal of biomedical materials research. Part B, Applied biomaterials* **2017**, 105, 1260; b) A. Gulec, M. A. Acar, B. K. Aydin, T. Demir, M. Ozkaya, *Proc Inst Mech Eng H* **2018**, 232, 1025; c) D. Bourell, B. Stucker, D. Espalin, K. Arcaute, D. Rodriguez, F. Medina, M. Posner, R. Wicker, *Rapid Prototyping Journal* **2010**; d) M. Winking, J. P. Stahl, M. Oertel, R. Schnettler, D. K. Boker, *Ger Med Sci* **2003**, 1, Doc08.
- [8] U. S. F. a. D. Administration, Filling in wrinkles safely, <https://www.fda.gov/consumers/consumer-updates/filling-wrinkles-safely>, accessed.
- [9] M. Silindir Gunay, Y. Ozer, *FABAD J Pharm Sci* **2009**, 34, 43.
- [10] a) G. Lewis, S. Mladsı, *Biomaterials* **1998**, 19, 117; b) M. Gonzalez-Andrades, R. Sharifi, M. M. Islam, T. Divoux, M. Haist, E. I. Paschalis, L. Gelfand, S. Mamodaly, L. Di Cecilia, A. Cruzat, F. J. Ulm, J. Chodosh, F. Delori, C. H. Dohlman, *Ocul Surf* **2018**, 16, 322.
- [11] A. S. Traish, J. Chodosh, *Semin Ophthalmol* **2010**, 25, 239.
- [12] a) T. Munker, S. van de Vijfeijken, C. S. Mulder, V. Vespasiano, A. G. Becking, C. J. Kleverlaan, G. CranioSafe, G. CranioSafe, A. G. Becking, L. Dubois, L. H. E. Karssemakers, D. M. J. Milstein, S. van de Vijfeijken, P. Depauw, F. W. A. Hoefnagels, W. P. Vandertop, C. J. Kleverlaan, T. Munker, T. J. J. Maal, E. Nout, M. Riool, S. A. J. Zaat, *J Mech Behav Biomed Mater* **2018**, 81, 168; b) R. M. Brinston, B. K. Wilson, *Med Device Technol* **1993**, 4, 18; c) D. W. Meltzer, *J Am Intraocul Implant Soc* **1981**, 7, 126.
- [13] S. Urano, I. Wakamoto, T. Yamakawa, *Mitsubishi Heavy Industries Technical Review* **2003**, 40, 1.
- [14] D. W. Plester, *Effects of radiation sterilization on plastics*, Duke Univ Press, United States **1973**.
- [15] L. K. Massey, in *The effect of sterilization methods on plastics and elastomers (second edition)* (Ed: L. K. Massey), William Andrew Publishing, U.S. **2005**, Ch. 3, p. 39.
- [16] A. Ashfaq, M.-C. Clochard, X. Coqueret, C. Dispenza, M. S. Driscoll, P. Ulański, M. Al-Sheikhly, *Polymers* **2020**, 12, 2877.
- [17] P. Tiwari, A. K. Srivastava, B. Q. Khattak, S. Verma, A. Upadhyay, A. K. Sinha, T. Ganguli, G. S. Lodha, S. K. Deb, *AIP Conference Proceedings* **2012**, 1447, 587.
- [18] R. A. Wach, H. Mitomo, F. Yoshii, T. Kume, *Macromolecular Materials and Engineering* **2002**, 287, 285.
- [19] a) R. Nathawat, A. Kumar, N. K. Acharya, Y. K. Vijay, *Surface and Coatings Technology* **2009**, 203, 2600; b) S. Lazare, R. Srinivasan, *The Journal of Physical Chemistry* **1986**, 90, 2124.
- [20] a) M. Żenkiewicz, M. Rauchfleisz, J. Czupryńska, J. Polański, T. Karasiewicz, W. Engelgard, *Applied Surface Science* **2007**, 253, 8992; b) R. L. Clough, K. Gillen, *Radiation-oxidation of polymers*, **1989**; c) N. W. Elshereksi, S. H. Mohamed, A. Arifin, Z. A. M. Ishak, **2014**, 25.

- [21] a) S. Barton, P. J. S. Foot, P. Tate, M. Kishi, B. Ghatora, *Polymers and Polymer Composites* **2013**, 21, 1; b) T. Kohnen, *J Cataract Refract Surg* **1996**, 22 Suppl 2, 1255; c) K. El-Salmawi, M. M. Abu Zeid, A. M. El-Naggar, M. Mamdouh, *Journal of Applied Polymer Science* **1999**, 72, 509.
- [22] a) L. H. Sperlin, in *Introduction to Physical Polymer Science*, Ch. 8, p. 349; b) S. Derbil, M. W. Khemici, N. Doulache, A. Gourari, N. Haine, *International Journal of Polymer Analysis and Characterization* **2017**, 22, 622.
- [23] ASTM, in *ASTM D790-17*, West Conshohocken, PA 2017.
- [24] C. Liu, T. Miyajima, G. Melangath, T. Miyai, S. Vasanth, N. Deshpande, V. Kumar, S. Ong Tone, R. Gupta, S. Zhu, D. Vojnovic, Y. Chen, E. G. Rogan, B. Mondal, M. Zahid, U. V. Jurkunas, *Proc Natl Acad Sci U S A* **2020**, 117, 573.
- [25] R. D. Glickman, *Eye Contact Lens* **2011**, 37, 196.
- [26] N. Rashi, K. Anil, Y. K. Vijay, presented at 2007 IEEE Particle Accelerator Conference (PAC), U.S., 25-29 June 2007, **2007**.
- [27] a) S. Mouaci, M. Saidi, N. Saidi-Amroun, in *Micro & Nano Letters*, Vol. 12, Institution of Engineering and Technology, 2017, 478; b) R. Dorati, M. Patrini, P. Perugini, F. Pavanetto, A. Stella, T. Modena, I. Genta, B. Conti, *Journal of Microencapsulation* **2006**, 23, 123.
- [28] a) S. Somodi, R. Guthoff, *Ophthalmologe* **1995**, 92, 452; b) S. Sharifi, M. M. Islam, H. Sharifi, R. Islam, P. H. Nilsson, C. H. Dohlman, T. E. Mollnes, E. I. Paschalis, J. Chodosh, *Translational Vision Science & Technology* **2020**, 9, 41.
- [29] a) L. M'Hamdi, N. M'Hamdi, N. M'Hamdi, DOI: 10.5772/53542 **2013**; b) G. Altankov, F. Grinnell, T. Groth, *J Biomed Mater Res* **1996**, 30, 385; c) R. E. Marchant, *The Journal of Adhesion* **1986**, 20, 211.
- [30] R. Sharifi, S. Mahmoudzadeh, M. M. Islam, D. Koza, C. H. Dohlman, J. Chodosh, M. Gonzalez-Andrades, *Adv. Mater. Interfaces* **2020**, 7, 1900767.
- [31] M. Gonzalez-Andrades, J. de la Cruz Cardona, A. M. Ionescu, A. Campos, M. Del Mar Perez, M. Alaminos, *Invest Ophthalmol Vis Sci* **2011**, 52, 215.
- [32] a) K. N. Ekdahl, J. D. Lambris, H. Elwing, D. Ricklin, P. H. Nilsson, Y. Teramura, I. A. Nicholls, B. Nilsson, *Adv Drug Deliv Rev* **2011**, 63, 1042; b) P. Schoengraf, J. D. Lambris, S. Recknagel, L. Kreja, A. Liedert, R. E. Brenner, M. Huber-Lang, A. Ignatius, *Immunobiology* **2013**, 218, 1.
- [33] a) J. M. Hackett, C. Ferguson, E. Dare, C. R. McLaughlin, M. Griffith, *Toxicol. in Vitro* **2010**, 24, 567; b) K. H. Chen, D. Azar, N. C. Joyce, *Cornea* **2001**, 20, 731.
- [34] a) S. Busschots, S. O'Toole, J. J. O'Leary, B. Stordal, *MethodsX* **2015**, 2, 8; b) P. W. Madden, J. N. Lai, K. A. George, T. Giovenco, D. G. Harkin, T. V. Chirila, *Biomaterials* **2011**, 32, 4076; c) S. I. Ivanova, S. Chakarov, A. Momchilova, R. Pankov, *Mater. Sci. Eng. C* **2017**, 78, 230.
- [35] M. M. Islam, R. Sharifi, S. Mamodaly, R. Islam, D. Nahra, D. B. Abusamra, P. C. Hui, Y. Adibnia, M. Goulamaly, E. I. Paschalis, A. Cruzat, J. Kong, P. H. Nilsson, P. Argueso, T. E. Mollnes, J. Chodosh, C. H. Dohlman, M. Gonzalez-Andrades, *Acta biomaterialia* **2019**, 96, 330.
- [36] G. Bergseth, J. K. Ludviksen, M. Kirschfink, P. C. Giclas, B. Nilsson, T. E. Mollnes, *Mol. Immunol.* **2013**, 56, 232.
- [37] T. E. Mollnes, T. Lea, S. S. Frøland, M. Harboe, *Scand. J. Immunol.* **1985**, 22, 197.